

# Thermally driven ballistic rectifier

J. Matthews,<sup>1</sup> D. Sánchez,<sup>2</sup> M. Larsson,<sup>3</sup> and H. Linke<sup>1,3</sup>

<sup>1</sup>*Physics Department and Materials Science Institute,  
University of Oregon, Eugene, Oregon 97403-1274*

<sup>2</sup>*Instituto de Física Interdisciplinar y Sistemas Complejos IFISC (CSIC-UIB), E-07122 Palma de Mallorca, Spain*

<sup>3</sup>*Solid State Physics and The Nanometer Structure Consortium (nmC@LU),  
Lund University, Box 118, S-221 00, Lund, Sweden*

The response of electric devices to an applied thermal gradient has, so far, been studied almost exclusively in linear response and in two-terminal devices. Here we present measurements of the response to a thermal bias of a four-terminal, quasi-ballistic junction with a central scattering site. We find a novel transverse thermovoltage measured across isothermal contacts. Using a multi-terminal scattering model, we show that the device's response to a thermal bias can be predicted from its nonlinear response to an electric bias. Our approach forms a foundation for the discovery and understanding of advanced, nonlocal, nonlinear thermoelectric phenomena that in the future may lead to novel thermoelectric device concepts.

PACS numbers: 72.20.Pa, 73.23.Ad, 73.40.Ei

Nanoelectronic devices with dimensions smaller than the characteristic scattering lengths for electrons are easily driven into the nonlinear regime, and show electron dynamics that depend on device symmetry. For instance, clear rectification effects have been observed in asymmetric microjunctions [1–3], quantum dots [4] and quantum point contact systems [5, 6]. These systems exhibit nonequilibrium effects that occur in the *nonlinear* regime of ballistic transport.

At the same time, there has been considerable progress in the use of mesoscopic conductors for thermoelectric devices such as nanoscale coolers and ultrasensitive thermometers [7]. At a more fundamental level, studies of heat flow in phase-coherent systems allow one to investigate basic properties of quantum transport when electric and thermal gradients act jointly on the same system [8]. Specifically, *thermoelectric* effects are observed when a voltage drop builds up in response to a temperature difference [9, 10]. Thus far, most of the literature has investigated thermopowers in two-terminal arrangements (for an exception see Ref. [11]), and in linear response. The latter point in particular is noteworthy as this is in contrast to electronics, where nonlinear devices such as diodes enable key functionalities.

Additionally, for the past four decades there has been sporadic research on so-called anisotropic thermoelectric materials. These are materials that exhibit off-diagonal elements in their electrical conductivity, thermal conductivity, or thermopower. Typically, anisotropic thermoelectrics comprise of either stacked multilayers of alternating materials [12, 13], or anisotropic crystalline materials [14]. Such systems, however, can only change the anisotropic properties of a given system by rotating the stacked multilayer or crystal orientation. This effectively limits the range of anisotropic properties that can be studied.

Here, we address transverse thermoelectric effects in

a quasi-ballistic device fabricated in a two-dimensional electron gas (2DEG), Fig. 1(a), which offers the great advantage that the scattering properties of the system can be controlled during fabrication. Specifically, we use a four-terminal microjunction with a central, asymmetric antidot to scatter electrons, Fig. 1(b), and perform thermoelectric measurements at a cryostat temperature of 0.75 K. In a similar device, previous observations have shown that a lateral AC *voltage* leads to a rectified, transverse response [1]. Here, we instead apply a lateral *temperature* difference across the junction through terminals 1 and 2, and observe a nonlocal thermovoltage between terminals 3 and 4, both of which are unheated. We note that similar thermovoltages have been detected previously in multi-terminal 2DEGs subjected to magnetic fields normal to the system (the Nernst effect [11, 15, 16]). In contrast to these works, the effect reported here is purely thermoelectric in nature and only

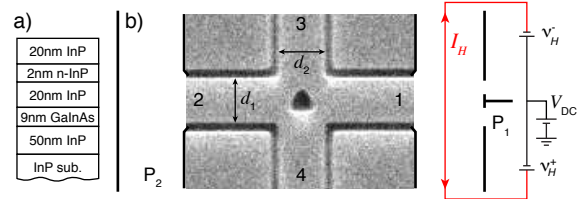


FIG. 1. (a) Schematic of the wafer structure with a 2DEG located in the GaInAs quantum well. (b) Schematic and SEM image of a four terminal antidot junction similar to the one reported on here. The lateral and transverse voltage drops are given by  $V_{12}$  and  $V_{34}$ , respectively. The actual four-terminal junction measured here had terminal widths of  $d_1 \approx 500$  nm and  $d_2 \approx 450$  nm, and an antidot with a base and height of about 550 nm and 380 nm, respectively. The side heating channels are 5  $\mu\text{m}$  wide, 30  $\mu\text{m}$  long, and  $\approx 4$   $\mu\text{m}$  from the scatterer (quasi-ballistic regime).

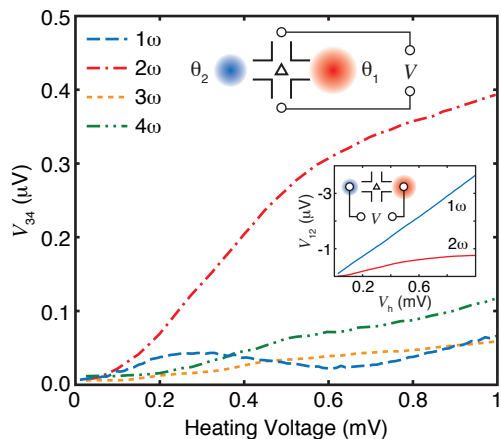


FIG. 2. (Main figure) First four harmonic transverse voltage responses to a temperature increase in terminal 1. (Top inset) Schematic of the measurement configuration. (Bottom inset) Measured lateral voltage drop across the junction during heating.

due to the symmetry breaking property of the central scatterer. Furthermore, we establish a theoretical model based on the multi-terminal scattering approach [17, 18] extended to the weakly nonlinear regime (up to quadratic order in voltage and linear order in temperature shifts) and show that we can predict the transverse thermoelectric response to a lateral thermal bias from measurements of the device's nonlinear response to an applied bias voltage.

Our device consists of an InP/Ga<sub>0.23</sub>In<sub>0.77</sub>As 2DEG wafer, see Fig. 1(a), patterned using the same techniques as in Ref. [19]. The antidot junction itself and its dimensions are shown in Fig. 1(b). Hall and Shubnikov de Haas measurements give a carrier concentration and mobility of  $2.93 \times 10^{-12} \text{ cm}^{-2}$  and  $1.16 \times 10^5 \text{ cm}^2/\text{Vs}$  respectively. The resulting mean free path,  $3.3 \text{ }\mu\text{m}$ , exceeds the characteristic length of the antidot region,  $0.5 \text{ }\mu\text{m}$ .

For our thermoelectric measurements, we are primarily interested in the transverse voltage response,  $V_{34} = V_3 - V_4$ , due to a change in the side terminal temperature(s), of either  $\theta_1$ ,  $\theta_2$ , or both. Here  $V_i$  and  $\theta_i$  are the shifts of the electrochemical potential and temperature in the  $i^{\text{th}}$  terminal away from the common electrochemical potential,  $\mu/e$ , and background cryostat temperature,  $\theta$ . To increase either  $\theta_1$  or  $\theta_2$ , we apply two 37 Hz heating currents, which have a relative phase of  $180^\circ$ , to the respective channel, see the circuit diagram in Fig. 1(b). Using  $P_1$  as a voltage probe, the amplitude of these signals could be tuned so that the resulting  $1\omega$  voltage at terminal 1 was minimized. Any remaining DC offset could have been minimized as well using a DC source to shift both heating voltages; however, no offset was needed.

In Fig. 2 we show results from an experiment where

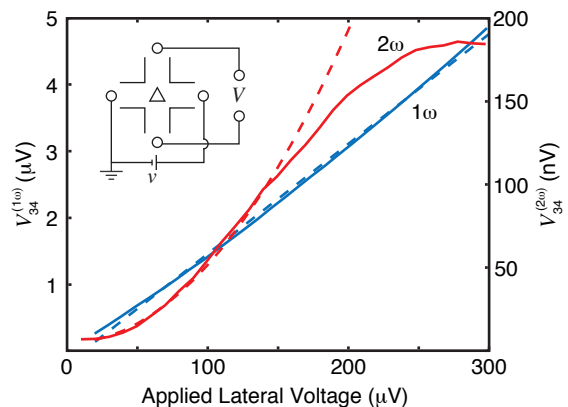


FIG. 3. 1<sup>st</sup> and 2<sup>nd</sup> harmonic transverse responses to a laterally applied 37 Hz voltage  $\nu$ . Also shown are linear and parabolic fits (dashed curves) to the  $1\omega$  and  $2\omega$  curves, respectively.

a temperature shift  $\theta_1$  was applied to terminal 1, and the first four harmonics of  $V_{34}$  were measured. Since the thermal gradient is generated from Joule heat, which is primarily proportional to the square of the applied heating voltage, the dominant  $2\omega$  response implies that the transverse response is linearly proportional to the applied temperature gradient,  $V_{34} \propto V_H^2 \propto \theta_1$ . We also measured the first and second harmonics of the lateral voltage drop  $V_{12}$  using the probes labeled  $P_1$  and  $P_2$  (see inset to Fig. 2). This voltage by itself is far too small to cause the observed transverse voltage, as can be seen from the device's measured  $1\omega$  and  $2\omega$  responses to an applied 37 Hz voltage, see Fig. 3.

$V_{34}$  in Fig. 2 is linear in  $\theta_1$  and can thus be interpreted as a thermovoltage. Remarkably, however, this thermovoltage is across two unheated contacts that, based on device geometry, can be assumed to be isothermal. We therefore propose that  $V_{34}$  is due to the difference between two or more thermovoltages in the junction. Sources of thermovoltages that are easily identifiable are the four quantum point contacts (QPC) defined by the antidot and the surrounding channel walls. In the general case of zero symmetry, each QPC thermovoltage would be unique, resulting in all four terminals being at different potentials. We will return to this interpretation below.

We can check the symmetry of our device by simply reversing the sign of the applied temperature differential. Given the intended left-right geometric symmetry of our antidot junction one may intuitively expect that  $V_{34}(\theta_1, \theta_2) = V_{34}(\theta_2, \theta_1)$ ; however, when the lateral temperature differential is reversed, measurements show a sign reversal in  $V_{34}$  (Fig. 4). Furthermore, when both terminals are heated simultaneously, the response tends toward zero.

We now aim to explain our results using the multi-

terminal thermoelectric scattering approach [17, 18] extended to the weakly nonlinear transport regime [20]. We consider a four-terminal junction with a central scatterer, as in Fig. 1(b), but without assuming any particular model for the scattering matrix. Based on the linear temperature and quadratic voltage responses shown in the experiment (see Figs. 2 and 3), we express the current  $I_\alpha$  through lead  $\alpha$  up to linear order in temperature and quadratic order in voltage differences,  $V_{\alpha\beta} = V_\alpha - V_\beta$ :

$$I_\alpha = \sum_{\beta \neq \alpha} [G_{\alpha\beta}(V_{\alpha\beta}) + M_{\alpha\beta}(V_{\alpha\beta})^2 + L_{\alpha\beta}(\theta_\alpha - \theta_\beta)]. \quad (1)$$

Importantly, Eq. (1) is manifestly gauge invariant, a property recently emphasized for mesoscopic rectifiers [21].

In the low temperature limit, the linear transport coefficients read,

$$G_{\alpha\beta} = \frac{2e^2}{h} t_{\alpha\beta}(\epsilon_F) \quad (2)$$

$$L_{\alpha\beta} = \frac{2\pi^2 e k_B^2 \theta}{3h} t'_{\alpha\beta}(\epsilon_F). \quad (3)$$

This approximation is valid provided the energy variation of the transmission probability,  $t_{\alpha\beta}$ , between leads  $\alpha$  and  $\beta$  is weak and the Fermi energy,  $\epsilon_F$ , is larger than the background temperature,  $\theta$ . This amounts to neglecting band edge effects. Hence, the transmission and its energy derivative,  $t'_{\alpha\beta}$ , are evaluated at  $\epsilon_F$ .

The leading order rectification term  $M_{\alpha\beta}$  is a complicated function of  $t'_{\alpha\beta}$  and of the transmission derivative  $\partial t_{\alpha\beta}(E, \{V_i\})/\partial V_\alpha|_{\text{eq}}$  evaluated at equilibrium [20]. Knowledge of the latter requires a self-consistent determination of the screening potential,  $U(\{V_i\})$ , inside the conductor. However, within a qualitative discussion we can neglect this term since it is proportional to the characteristic potential,  $u_\alpha = (\partial U/\partial V_\alpha)|_{\text{eq}}$  [20], whose strength can be estimated within mean-field theory from  $u \sim C_\mu/C$ , where  $C_\mu^{-1} = (e^2 D)^{-1} + C^{-1}$ ,  $C$  is a capacitance coefficient that measures interactions, and  $D$  denotes the density of states associated with the scattering states. In widely open systems one has  $C \gg e^2 D$  (non-interacting limit), and the rectification term becomes

$$M_{\alpha\beta} \simeq -\frac{e^3}{h} t'_{\alpha\beta}(\epsilon_F). \quad (4)$$

To find  $V_{34}$  as a function of the lateral voltages ( $V_1$  and  $V_2$ ) and temperatures ( $\theta_1$  and  $\theta_2$ ) we recall that terminals 3 and 4 act as voltage probes. We then solve the two conditions  $I_3 = I_4 = 0$  with the aid of Eq. (1) in the cold isothermal case ( $\theta_3 = \theta_4 = 0$ ). For definiteness, we neglect the products  $V_i V_{(3,4)}$  since in our experiment,  $V_{34}$  is much smaller than  $V_{12}$ . Then,

$$V_{34} = A(V_1 - V_2) + \sum_{j=1,2} B_j(g_\theta \theta_j - g_e V_j^2), \quad (5)$$

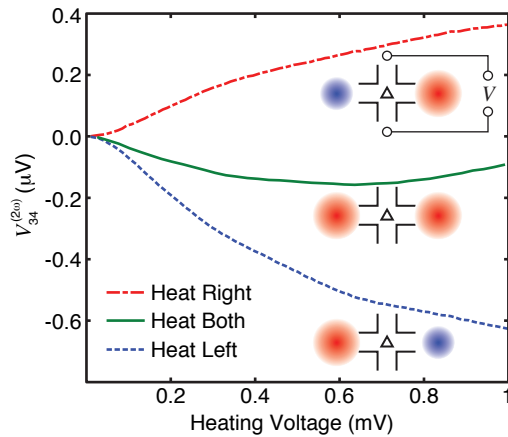


FIG. 4.  $2\omega$  transverse response due to heating both side channels simultaneously and individually.

where we have defined,

$$A = \frac{t_{31}t_{42} - t_{41}t_{32}}{D}, \quad (6)$$

$$B_j = \frac{(t_{41} + t_{42})t'_{3j} - (t_{31} + t_{32})t'_{4j}}{D}, \quad (7)$$

with  $D = (t_{31} + t_{32})(t_{41} + t_{42}) + t_{34}(t_{41} + t_{42}) + t_{43}(t_{31} + t_{32})$ . Here  $g_e = e/2$  and  $g_\theta = \pi^2 k_B^2 \theta/3e$ .

Interestingly, Eq. 5 predicts that the coefficients  $B_j$  that describe the transverse response to an applied temperature differential also describe its response to the square of an applied voltage.

In an ideal device with perfect left-right symmetry, Eq. (6) predicts  $A = 0$ , leaving the quadratic terms described by  $B_j$  to be the leading order response. Any non-zero value of  $A$ , therefore, can indicate left-right asymmetries in the junction. We can determine  $A$  and  $B_1$  for our system by fitting Eq. (5) to the applied voltage data, for  $V_{12} < 100 \mu\text{V}$ , in Fig. 3. Fitting these measurements yields  $A = -1.43 \times 10^{-2}$  and  $B_1 = 2.07 \times 10^{20} \text{ J}^{-1}$ .

We would like to extract the transverse thermopower  $S_{34,12}$  from the measurements in Fig. 2. Ideally we would simply divide  $V_{34}$  by  $\theta_1$ ; however, our device layout does not allow direct measurement of  $\theta_1$ . Instead, we analyze the first and second harmonic measurements of  $V_{34}(V_h)$  and  $V_{12}(V_h)$  in Fig. 2 using  $A$ ,  $B_1$ , and Eq. (5). We first approximate the temperature rise in terminal 1 as  $\theta_1 = a_1 V_H + a_2 V_H^2$ , where  $V_H = V_h \cos(\omega t)$ . Our goal is to estimate  $\theta_1$  by determining  $a_1$  and  $a_2$ . From the data in Fig. 2, we can also write down fit equations for  $V_{12}(V_h)$  and  $V_{34}(V_h)$ :  $V_{12} = (-3.63 \times 10^{-3})V_h \cos(\omega t) + (-5.28V^{-1})V_h^2 \cos(2\omega t)$  and  $V_{34} = (-1.4 \times 10^{-4})V_h \cos(\omega t) + (3.7V^{-1})V_h^2 \cos(2\omega t)$ . Here we have limited our fits to  $V_h \leq 150 \mu\text{V}$ . Inserting these three equations into Eq. 5, using the values for  $A$  and  $B_1$  determined above, and identifying the first and second harmonic terms, gives two equations we can use

to determine  $a_1$  and  $a_2$ . We find  $a_1 = -320$  K/V and  $a_2 = 1.2 \times 10^7$  K/V<sup>2</sup>. At  $V_h = 150$   $\mu$ V, these values give a temperature rise of  $\theta_1 = 220$  mK and a thermopower of  $S_{34,12} = 0.36$   $\mu$ V/K.

Based on our considerations above, and on Eq. (5), we interpret the transverse thermopower as the difference between two QPC thermopowers. For comparison, the difference between two QPC thermopowers is given by

$$\Delta S^{QPC} = \frac{k_B \ln(2)}{e} \left( \frac{1}{N_T - 0.5} - \frac{1}{N_B - 0.5} \right), \quad (8)$$

where  $N_{(T,B)} \geq 1$  represent the integer number of conductance modes in the effective top and bottom QPCs. We can estimate the  $N$  values for our system from conductance measurements of the junction.

If we assume that the junction is symmetric as intended,  $t_{13} = t_{23}$  and  $t_{14} = t_{24}$ , then  $N_{12}^{eff} = (N_T + N_B)/2$ , where  $N_{12}^{eff} = G_{12}/gT$  is the effective number of modes between terminals 1 and 2. Here  $G_{12} = 8.73 \times 10^{-4} \Omega^{-1}$  is a two-terminal conductance measurement between terminals 1 and 2,  $g = 2e^2/h$  is the conductance quantum, and the fitting parameter  $T$  is the transmission probability. One approximate solution to  $\Delta S^{QPC} \approx S_{34,12}$  is  $N_T = 13$ ,  $N_B = 14$ , and  $T = 0.83$ , which gives  $\Delta S^{QPC} = 0.35$   $\mu$ V. Therefore the observed magnitude of  $S_{34,12}$  agrees well with what is expected based on the model of two QPC thermopowers.

Finally, we discuss the sign reversal upon exchange of the thermal shifts observed in Fig. 3. We focus on temperature differences only and thus set  $V_1 = V_2 = 0$  in Eq. 5. The  $2\omega$  response can be decomposed into components that are symmetric,  $S_{34}^S$ , and antisymmetric,  $S_{34}^A$ , under the transformation  $(\theta_1, \theta_2) \rightarrow (\theta_2, \theta_1)$ :

$$V_{34} = S_{34}^S \frac{\theta_1 + \theta_2}{2} + S_{34}^A \frac{\theta_1 - \theta_2}{2}, \quad (9)$$

where  $S_{34}^S = B_1 + B_2$  and  $S_{34}^A = B_1 - B_2$ . When both terminals are heated simultaneously and equally, the main contribution stems from the symmetric component, which is generally nonzero. When  $\theta_1$  and  $\theta_2$  are not equal and exchanged, the symmetric component remains unchanged while the antisymmetric component reverses sign. Note that  $S_{34}^A$  exists only for scatterers showing some kind of asymmetry in the transmission derivative coefficients ( $t'_{31} \neq t'_{32}$  or  $t'_{41} \neq t'_{42}$ ). Based on the data in Fig. 4, we believe our junction has a strong antisymmetric component and weak symmetric component. We attribute this thermopower asymmetry to unintentional scattering asymmetries of the junction channels between terminal 3 or 4 and the side leads.

We have shown that a four-terminal junction with a symmetry-breaking scatterer can be used to generate a thermovoltage between two cold isothermal contacts. We have put forward a simple noninteracting model for

multi-terminal thermoelectric transport that accounts for most observed effects. Given the great control over device geometry and symmetry afforded by nanofabricated devices, our approach can be used to explore advanced thermoelectric functionalities — such as electronic thermal rectifiers or more efficient thermoelectric energy converters — due to the opportunity to separate heat and charge flow in multi-terminal devices.

We acknowledge Hongqi Xu of Lund University for fruitful discussions, and financial support from NSF IGERT grant No. DGE-0549503, the National Science Foundation Grant No. DGE-0742540, ARO Grant No. W911NF0720083, the Air Force Office of Scientific Research, Air Force Material Command, USAF grant number FA8655-11-1-3037, Energimyndigheten Grant No. 329201, MICINN Grant No. FIS2008-00781, nmC@LU, and the Foundation for Strategic Research (SSF).

- 
- [1] A. M. Song, A. Lorke, A. Kriele, J. P. Kotthaus, W. Wegscheider, and M. Bichler, *Phys. Rev. Lett.* **80**, 3831 (1998).
  - [2] S. de Haan, A. Lorke, J. P. Kotthaus, W. Wegscheider, and M. Bichler, *Phys. Rev. Lett.* **92**, 056806 (2004).
  - [3] B. Hackens, L. Gence, S. Faniel, C. Gustin, X. Wallart, S. Bollaert, A. Cappy, and V. Bayot, *Physica E* **34**, 515 (2006).
  - [4] H. Linke, W. Sheng, A. Löfgren, H. Xu, P. Omling, and P. E. Lindelof, *Europhys. Lett.* **44**, 341 (1998).
  - [5] H. Linke *et al.*, *Science* **286**, 2314 (1999).
  - [6] I. Shorubalko, H. Q. Xu, I. Maximov, P. Omling, L. Samuelson, and W. Seifert, *Appl. Phys. Lett.* **79**, 1384 (2001).
  - [7] F. Giazotto, T. T. Heikkilä, A. Luukanen, A. M. Savin, and J. P. Pekola, *Rev. Mod. Phys.* **78**, 217 (2006).
  - [8] Y. Dubi and M. Di Ventra, *Rev. Mod. Phys.* **83**, 131 (2011).
  - [9] L. W. Molenkamp, H. van Houten, C. W. J. Beenakker, R. Eppenga, and C. T. Foxon, *Phys. Rev. Lett.* **65**, 1052 (1990).
  - [10] S. F. Godijn, S. Möller, H. Buhmann, L. W. Molenkamp, and S. A. van Langen, *Phys. Rev. Lett.* **82**, 2927 (1999).
  - [11] A. G. Pogosov *et al.*, *Phys. Rev. B* **66**, 201303 (2002).
  - [12] V. P. Babin *et al.*, *Sov. Phys. Semicond.* **8**, 478 (1974).
  - [13] A. Kyarad and H. Lengfellner, *Appl. Phys. Lett.* **85**, 5613 (2004).
  - [14] T. Zahner *et al.*, *Europhys. Lett.* **40**, 673 (1997).
  - [15] S. Maximov, M. Gbordzoe, H. Buhmann, L. W. Molenkamp, and D. Reuter, *Phys. Rev. B* **70**, 121308 (2004).
  - [16] S. Goswami, C. Siegert, M. Pepper, I. Farrer, D. A. Ritchie, and A. Ghosh, *Phys. Rev. B* **83**, 073302 (2011).
  - [17] M. Büttiker, *Phys. Rev. Lett.* **57**, 1761 (1986).
  - [18] P. N. Butcher, *J. Phys. Cond. Matter* **2**, 4869 (1990).
  - [19] M. Larsson, D. Wallin, and H. Q. Xu, *J. Appl. Phys.* **103** (2008).
  - [20] T. Christen and M. Büttiker, *Europhys. Lett.* **35**, 523 (1996).
  - [21] M. Büttiker and D. Sánchez, *Phys. Rev. Lett.* **90**, 119701 (2003).